

A New Modular Motor–Modular Inverter Concept for Medium-Voltage Adjustable-Speed Drive Systems

Ekrem Cengelci, *Student Member, IEEE*, Prasad N. Enjeti, *Fellow, IEEE*, and James W. Gray, *Associate Member, IEEE*

Abstract—In this paper, a new modular motor–modular inverter concept for medium-voltage adjustable-speed drive (MV-ASD) systems is introduced. It is shown that standard MV motor winding connections can be reconnected into several three-phase groups, each powered by a separate three-phase pulsewidth modulation inverter, resulting in a high-performance MV-ASD system. The proposed approach is fault tolerant and can continue to operate at reduced power levels, under inverter and/or motor faults. An example 250-hp four-pole 60-Hz 2300-V/4160-V motor winding connection diagram along with the associated inverter configurations is analyzed. Results from analysis are presented on the aspects of faults and motor operation under partial winding excitation. Experimental results on a low-voltage (460 V) 10-hp ASD are demonstrated.

Index Terms—Adjustable-speed drive, modular motor–modular inverter.

I. INTRODUCTION

MEDIUM-VOLTAGE adjustable-speed drive (MV-ASD) systems offer significant advantages in fan, pump, and process control applications in terms of high efficiencies and high performance [1]–[5]. The application of these high-power MV-ASD's is, in general, associated with critical process areas of the plant and any shutdown of the system could result in a major process upset and loss of production [6].

In order to improve reliability of such systems, six-phase induction motors fed by double current-source inverters (CSI's) have come into existence [2], [4], [5], [7], [8]. Further, [9] presents an extensive investigation of an n -phase induction motor drive system powered by n independent single-phase inverters. Such a system requires a specially wound multiphase motor, each phase powered by a single phase-inverter unit. Although failure of any one phase-drive unit does degrade motor performance somewhat, the urgency of immediate repairs is reduced since the system shutdown is not required.

The approach in [9] for achieving improved reliability can be termed a modular motor–modular inverter (MM-MI) concept. In this paper, the MM-MI concept is further extended for standard three-phase induction motors (Fig. 1). It is shown that

Paper IPCSD 99–101, presented at the 1999 Industry Applications Society Annual Meeting, Phoenix, AZ, October 3–7, and approved for publication in the IEEE TRANSACTIONS ON INDUSTRY APPLICATIONS by the Industrial Drives Committee of the IEEE Industry Applications Society. Manuscript submitted for review June 1, 1999 and released for publication January 22, 2000.

E. Cengelci and P. N. Enjeti are with the Power Electronics and Power Quality Laboratory, Department of Electrical Engineering, Texas A&M University, College Station, TX-77843-3128 USA (e-mail: cengelci@ee.tamu.edu; enjeti@tamu.edu).

J. W. Gray is with the Industrial Division, Toshiba International Corporation, Houston, TX 77041 USA.

Publisher Item Identifier S 0093-9994(00)04400-5.

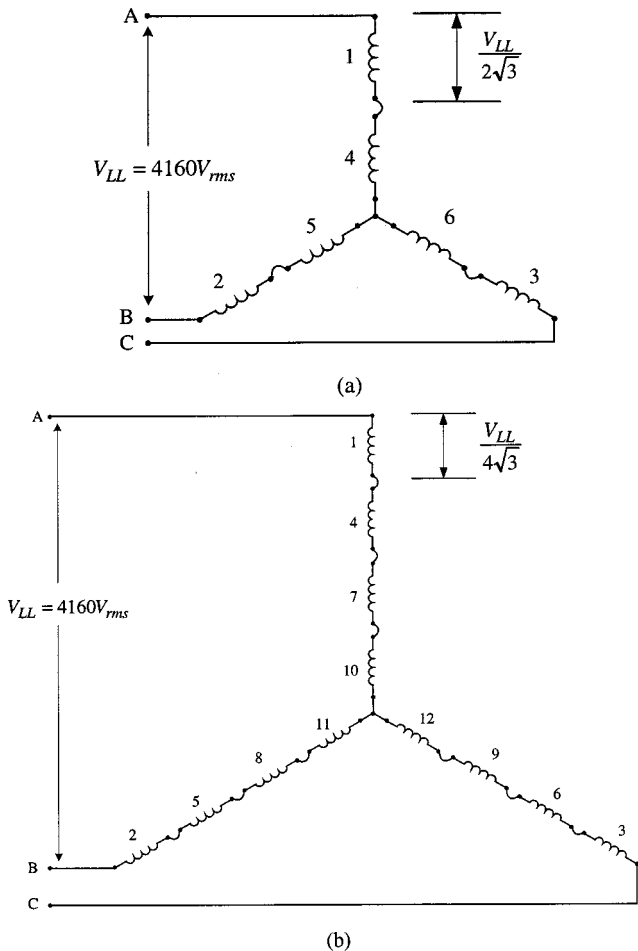


Fig. 1. Winding diagrams of commercially available medium-voltage induction motors. (a) Winding diagram of a two-pole medium-voltage induction motor. (b) Winding diagram of a four-pole medium-voltage induction motor.

standard (medium voltage) motor winding connections can be reconnected into several three-phase groups, each powered by a separate three-phase pulsewidth modulation (PWM) inverter, resulting in a high-performance MV-ASD system (Fig. 2). The proposed approach has the following advantages.

- 1) The proposed modular approach (MM-MI) achieves a higher level of reliability due to its inherent redundancy.
- 2) The modular concept facilitates the use of lower voltage insulation systems both in the motor and in inverter construction. Further, lower voltage semiconductor devices are employed in the inverters and no high-voltage insulation requirements need to be met within the inverter modules. These two features translate into significant cost savings.

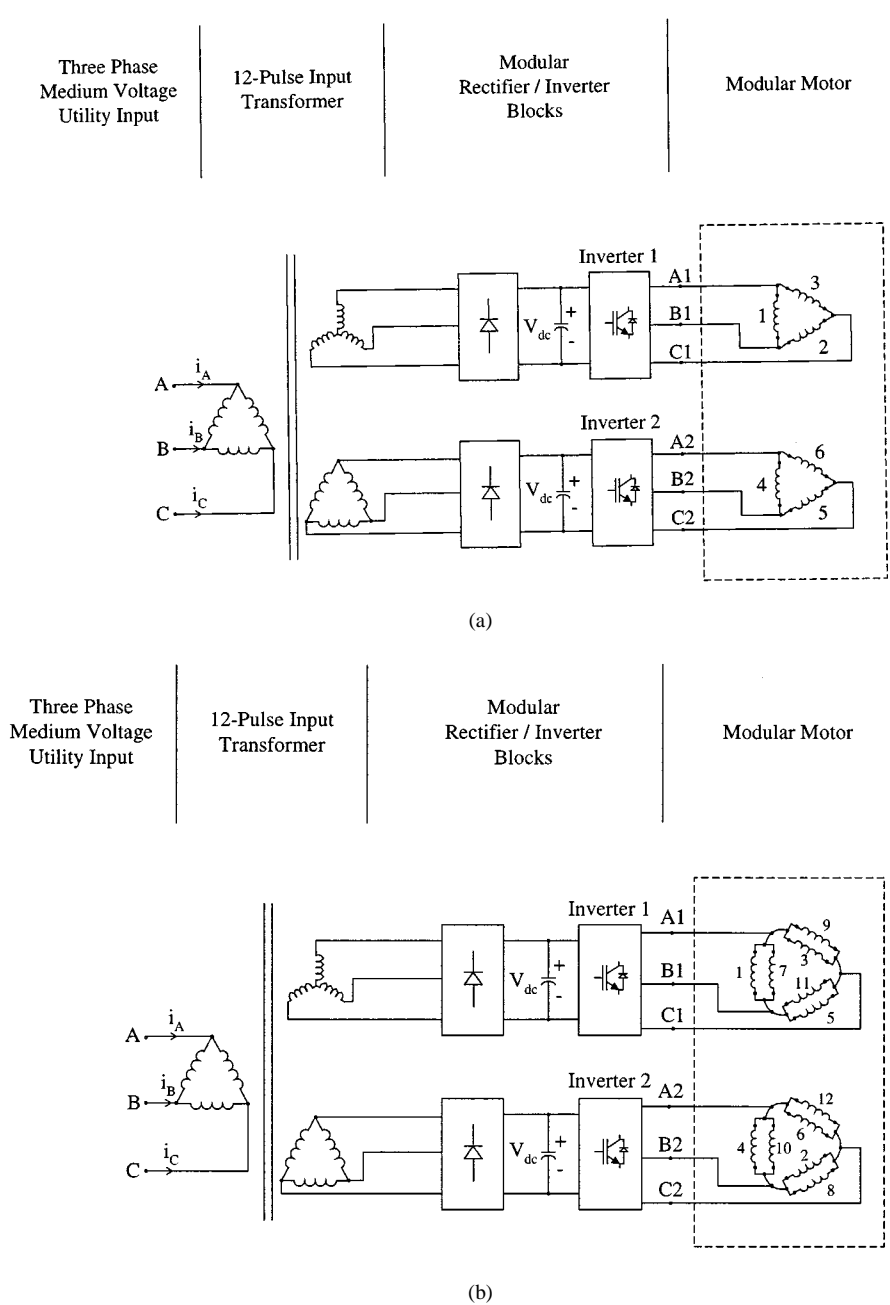


Fig. 2. (a) Complete MV-ASD for six-lead MM-MI approach along with a 12-pulse input transformer for clean input (the motor is two-pole). (b) Complete MV-ASD for six-lead MM-MI approach along with a 12-pulse input transformer for clean input (the motor is four-pole).

- 3) By proper selection of motor coil groups and the inverter connections, torque ripple can be kept at acceptable levels under fault conditions.
- 4) Modular inverter construction facilitates easy maintenance and spare management.
- 5) The proposed approach facilitates complete bypass of the inverter and allows the motor to be run directly on utility supply in the event of an inverter failure.
- 6) The proposed approach requires access to motor winding terminals and, therefore, is most suitable for new installations.

connections. A six-lead connection, shown in Fig. 2, powers the motor by two separate three-phase PWM inverters operating in master/slave mode. Further, a 12-lead connection requires four separate three-phase PWM inverters to power the motor (Fig. 3). Results from analysis are presented on the aspects of faults and motor operation under partial winding excitation.

II. WINDING CONNECTIONS OF COMMERCIALY AVAILABLE MV INDUCTION MOTORS

This paper examines how the winding connections of a commercially available 250-hp four-pole 60-Hz 2300-V/4160-V induction motor can be reconnected into six-lead and twelve-lead

Winding connections of commercially available two-pole and four-pole MV induction motors are shown in Fig. 1(a) and (b), respectively. For example, the winding labeled as 1 in Fig. 1(a),

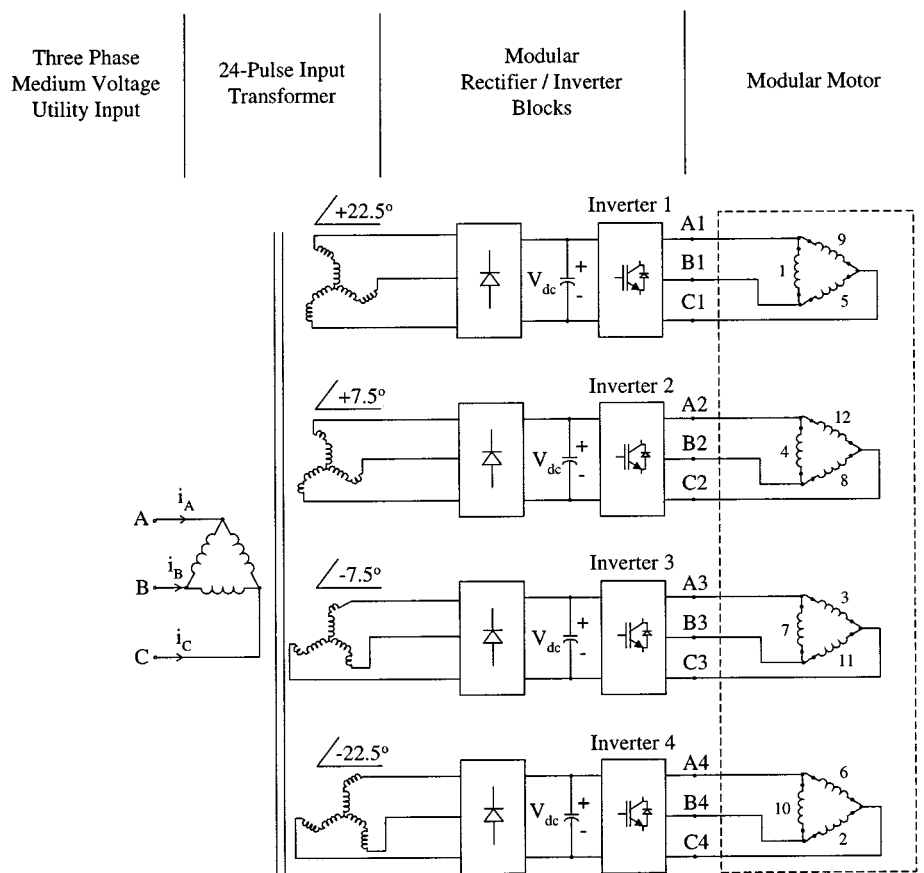


Fig. 3. Complete MV-ASD for 12-lead MM-MI approach along with a 24-pulse input transformer for clean input power.

is referred to as a “coil group” and it may be comprised of many coils connected in series depending on the number of slots and winding pattern (lap winding or concentrated winding) of the motor. The two-pole motor in Fig. 1(a) has two coil groups on each phase and total of six coil groups, whereas the four-pole motor in Fig. 1(b) has four coil groups on each phase and total of 12 coil groups. In general, the number of coil groups on each phase of the MV induction motor is equal to the pole number of the motor.

The windings of the MV motors are connected in star as shown in Fig. 1(a) and (b) for $4160\text{-}V_{\text{rms}}$ across the motor terminals A, B and C, whereas they are connected in delta for $2300\text{-}V_{\text{rms}}$ applied to the motor terminals.

III. PROPOSED MM-MI APPROACH FOR MV-ASD

The proposed MM-MI approach is grouped under two categories: 6-lead approach and twelve-lead approach. The 6-lead approach is suitable for MV motors with any number of poles and the 12-lead approach is suitable for motors with pole numbers of multiples of four (four-pole, eight-pole, etc.)

A. Six-Lead MM-MI ASD Concept

Fig. 2(a) shows the complete MV MM-MI ASD with the two-pole motor [Fig. 1(a)] connected in six-lead. One coil group from each phase of the motor [Fig. 1(a)] is taken and connected in delta as shown in Fig. 2(a). Since we have two coil groups

on each phase of the motor, we have two delta-connected motor coils in Fig. 2(a). This connection is referred to as a six-lead connection in this paper, since we have six leads available at the motor terminals. Two delta-grouped motor windings are now connected to two three-phase inverters as shown in Fig. 2(a). Inverters 1 and 2 in Fig. 2(a) have to be synchronized with each other so that line-to-line output voltage patterns of the two inverters are identical. The voltage rating of each motor coil group in Fig. 1(a) is

$$V_a = \frac{V_{LL}}{2\sqrt{3}} \quad (1)$$

This is also the output voltage rating of each inverter (Fig. 2(a)). Therefore, the proposed six-lead connection [Fig. 2(a)] effectively reduces the required inverter/motor voltage rating by 71%. For an example MV motor of $V_{LL} = 4160\text{ V}$ arranged in a six-lead configuration [Fig. 2(a)], two inverters with rated output voltage of 1200 V are required. More details are illustrated in Section VI.

Two three-phase inverters can be connected on the same dc bus or the three-phase diode rectifiers can be connected to the same secondary winding of the input transformer since delta 1 and delta 2 of the motor windings in Fig. 2(a) are electrically isolated from each other. Therefore, the purpose of the 12-pulse input transformer in Fig. 2(a) is to realize higher quality utility input current.

Alternatively, a four-pole motor shown in Fig. 1(b) can also be connected in six-lead configuration as shown in Fig. 2(b). The 12 coil groups in Fig. 1(b) are grouped in two deltas as shown in Fig. 2(b).

B. Twelve Lead MM-MI, ASD Concept

Fig. 3 shows the complete MV MM-MI ASD with the four-pole motor [Fig. 1(b)] connected in 12-lead. One coil group from each phase of the motor [Fig. 1(b)] is taken and connected in delta as shown in Fig. 3. Since we have four coil groups on each phase of the motor, we have four delta-connected motor coil groups in Fig. 3. Since we have 12 leads available at the motor terminals, this connection is referred to as a 12-lead connection in this paper. Four delta-grouped motor windings are connected to four three-phase inverters as shown in Fig. 3. All four inverters in Fig. 3 have to be synchronized with each other so that line-to-line output voltage patterns of all four inverters are identical. The voltage drop across each motor coil group in Fig. 1(b) is

$$V_a = \frac{V_{LL}}{4\sqrt{3}}. \quad (2)$$

This is also the output voltage rating of each inverter (Fig. 3). Therefore, the proposed six-lead connection (Fig. 3) effectively reduces the required inverter/motor voltage rating by 85.6%. For an example MV motor of $V_{LL} = 4160$ V arranged in a 12-lead configuration (Fig. 3), four inverters with rated output voltage of 600 V are required. Alternatively, the 6-lead configuration in Fig. 2(b) can be adopted with two 600-V inverters. More details are illustrated in Section VI.

MV motors with pole numbers of multiples of four (four-pole, eight-pole, 12-pole, etc.) can be connected in 12-lead connection by grouping motor coil groups in total of four delta-connected motor windings.

The connections to group the motor windings in several deltas can be made inside the motor without bringing all coil group terminals outside the motor. Therefore, 6-lead and 12-lead configurations require only 6 and 12 leads to be brought to the motor terminals, respectively. MV motors normally have from 6 to 12 leads available at the motor terminals for soft-start purposes (e.g., part winding startup and star-delta startup.) Hence, the proposed configurations may not drastically affect the motor size or motor terminal box size.

IV. ANALYSIS

In this section, the MMF analysis of an example 250-hp four-pole 60-Hz 2300-V/4160-V commercially available induction motor is presented in detail. The analysis facilitates detailed evaluation of 6-lead and 12-lead configurations under normal and fault conditions.

A. MMF Analysis of a Four-Pole MV Motor

A simplified winding diagram of the MV induction motor is shown in Fig. 4. The motor in Fig. 4 has 60 slots and is lap wound. It is a four-pole motor so that it has 12 coil groups in total (four coils per phase) and each coil is comprised of five

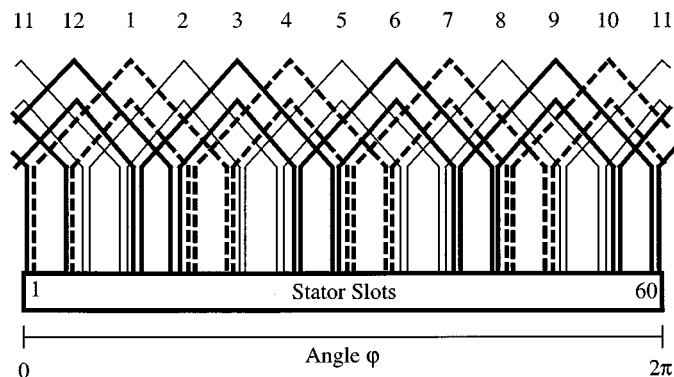


Fig. 4. Simplified winding diagram of the example four-pole 250-hp 2300/4160-V induction motor.

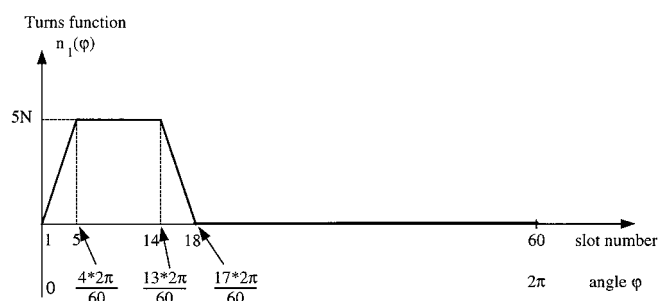


Fig. 5. Turns function of coil group 1 in Fig. 4.

series-connected coils. The coil groups with the same line style in Fig. 4 belong to the same phases. The coil groups in Fig. 4 are numbered from 1 to 12 as shown. The 12 coil groups of the motor labeled in Figs. 1(b) and 3 are also depicted in Fig. 4 to show their respective positions in the stator slots. The labeling of the coil groups in Fig. 4 is not random and its order is explained in Section IV-B. It is assumed in the MMF analysis that the motor magnetics are linear. The MMF analysis of the example motor (Figs. 1(b) and 4) discussed in this section applies to any four-pole induction motor with 12 coil groups, regardless of its winding style and stator slot number. One could follow a similar approach for motors with different winding configurations.

The turns function $n_1(\varphi)$ of coil group 1 (Fig. 4) is shown in Fig. 5. Let us assume that each coil group is comprised of five coils in series of N turns each. Therefore, the magnitude of the turns function in Fig. 5 is $5N$. The winding function [12] $N_1(\varphi)$ is defined as the ac component of turns function $n_1(\varphi)$. Therefore,

$$N_1(\varphi) = n_1(\varphi) = \langle n_1(\varphi) \rangle \quad (3)$$

where $\langle n_1(\varphi) \rangle$ is the average value of $n_1(\varphi)$.

Also, for the given motor, the coil groups next to each other are apart from each other by $\varphi = 30^\circ$. Therefore, the turns functions of coil groups next to each other have the same shape as of $n_1(\varphi)$ and are 30° apart. Therefore, the winding function of n th coil group can be expressed as follows:

$$N_n(\varphi) = (-1)^{n+1} \cdot N_1(\varphi - (n-1) \cdot 30^\circ) \quad (4)$$

TABLE I
FOURIER SERIES COMPONENTS OF $N_1(\varphi)$ IN (5)

h	A_h	α_h
1	1.988N	-51°
2	1.512N	-102°
3	0.884N	-153°
4	0.287N	-204°
5	0.136N	-75°
6	0.325N	-126°
7	0.308N	-177°
8	0.176N	-228°

where n represents coil group number (1–12). From Fig. 5 and (3) and $n = 1$, the Fourier series of winding function for coil group 1 can be expressed as

$$N_1(\varphi) = \sum_{h=1}^{\infty} A_h \cos(h\varphi + \alpha_h). \quad (5)$$

The coefficients A_h and α_h are given in Table I with respect to harmonic order $h = 1$ –8.

Since the MMF generated by coil group 1 is defined as its winding function, multiplied by the current $i_1(t)$, $MMF_1(t, \varphi)$ can be expressed as follows:

$$MMF_1(t, \varphi) = i_1(t) \cdot N_1(\varphi). \quad (6)$$

The resulting total MMF due to the excitation of motor coils is given by

$$MMF(t, \varphi) = \sum_{n=1}^{12} MMF_n(t, \varphi) = \sum_{n=1}^{12} i_n(t) \cdot N_n(\varphi) \quad (7)$$

where $i_n(t)$ is the current through coil group n . Assuming balanced currents are flowing in the motor coil groups, the currents of 12 coil groups are given by

$$\begin{aligned} i_1(t) &= i_4(t) = i_7(t) = i_{10}(t) = I \sin(\omega t) \\ i_3(t) &= i_6(t) = i_9(t) = i_{12}(t) = I \sin(\omega t - 120^\circ) \\ i_2(t) &= i_5(t) = i_8(t) = i_{11}(t) = I \sin(\omega t - 120^\circ). \end{aligned} \quad (8)$$

Substituting (8) into (7), we have

$$\begin{aligned} MMF(t, \varphi) &= I \sin(\omega t) \cdot [N_1(\varphi) + N_4(\varphi) + N_7(\varphi) + N_{10}(\varphi)] \\ &\quad + I \sin(\omega t - 120^\circ) \\ &\quad \cdot [N_3(\varphi) + N_6(\varphi) + N_9(\varphi) + N_{12}(\varphi)] \\ &\quad + I \sin(\omega t - 120^\circ) \\ &\quad \cdot [N_2(\varphi) + N_5(\varphi) + N_8(\varphi) + N_{11}(\varphi)]. \end{aligned} \quad (9)$$

From (4) and (9), we have

$$\begin{aligned} MMF(t, \varphi) &= I \sin(\omega t) \cdot [N_1(\varphi) + N_1(\varphi - 90^\circ) + N_1(\varphi - 180^\circ) \\ &\quad - N_1(\varphi - 270^\circ)] + I \sin(\omega t - 120^\circ) [N_1(\varphi - 60^\circ) \\ &\quad - N_1(\varphi - 150^\circ) + N_1(\varphi - 240^\circ) - N_1(\varphi - 330^\circ)] \\ &\quad + I \sin(\omega t + 120^\circ) \cdot [-N_1(\varphi - 30^\circ) + N_1(\varphi - 120^\circ) \\ &\quad - N_1(\varphi - 210^\circ) + N_1(\varphi - 300^\circ)]. \end{aligned} \quad (10)$$

Substituting (5) into (10) and after some simplification it can be deduced that $MMF(t, \varphi)$ has terms of $\sin(\omega t + h\varphi + \alpha_h)$ and

$\sin(\omega t - h\varphi - \alpha_h)$. The MMF components of sine terms with $+h\varphi$ and $-h\varphi$ rotate in opposite directions. If we assume the MMF components of sine terms with $+h\varphi$ as rotating in positive direction, the ones with $-h\varphi$ rotate in negative direction.

The respective MMF components of (10) for $h = 1$ –3 are shown in Fig. 6. It can be seen from Fig. 6(a) and (c) that the resultant positive-direction rotating and negative-direction rotating components of the MMF for $h = 1$ and 3 add to zero. For $h = 2$, the resultant MMF components of $+2\varphi$ terms add to zero and only -2φ terms remain. Therefore, (10) simplifies to

$$MMF(t, \varphi) = 9.072 \cdot I \cdot N \cdot \sin(\omega t - 2\varphi + 180^\circ). \quad (11)$$

It is clear from the above analysis and from (10), (11), and Fig. 6 that resultant MMF is nearly sinusoidal and repeats itself twice for angle $\varphi = 0$ to 2π . The procedure established in this section facilitates the motor MMF analysis for partial winding excitation.

B. Selection Criteria for Motor Coil Groups in Six-Lead and 12-Lead Connections

Equation (10) depicts the overall MMF of the motor due to the excitation of various coil groups shown in Fig. 4. Now, under fault conditions, a certain portion of motor windings are not excited due to inverter/motor faults. Under this condition, it is important to properly group the motor coils such that the resulting MMF under partial winding excitation has the least possible harmonic components. This can be achieved by proper grouping of the coil groups as follows. For the example four-pole motor winding (Fig. 4), Fig. 6 shows both positive-direction and negative-direction rotating MMF components for $h = 1$ –3. From Fig. 6, for a 12-lead connection, selecting coil groups 1, 5, 9; 2, 6, 10; 3, 7, 11; and 4, 8, 12 would yield the optimum result. This 12-lead coil grouping selection is depicted in Fig. 3. Now, if, for example, the inverter 1 powering coil groups 1, 5, 9 were to fail (coil groups 1, 5, 9 were not energized), then from Fig. 6 it is clear that MMF harmonic components with $+\varphi$ terms [$h = 1$ in Fig. 6(a)] are not cancelled and the fundamental MMF component [$h = 2, -2\varphi$ terms in Fig. 6(b)] decreases by 25%. However, all other MMF vector components due to the loss of 1, 5, 9 coil groups remain cancelled. Therefore, the suggested coil grouping yields the minimum possible MMF harmonics in case of the failure of one of the inverters in Fig. 3.

The best coil grouping for the six-lead configuration is such that the coil groups 1, 3, 5, 7, 9, 11 are powered by inverter 1 and the remaining coil groups of 2, 4, 6, 8, 10, 12 are powered by inverter 2 as depicted in Fig. 2(b). Now, if inverter 1 in Fig. 2(b) were to fail, it is clear from Fig. 6 that -2φ terms [$h = 2$, Fig. 6(b)] decrease by 50% and all other remaining vectors are still cancelled among themselves. Therefore, this selection of coil groups is the best since it results in minimum possible MMF harmonics under partial winding excitation.

C. Corrective Measures

From the above discussion and Fig. 6, loss of inverter 1 results in coil groups 1, 5, 9 being deenergized and contributes to a pul-

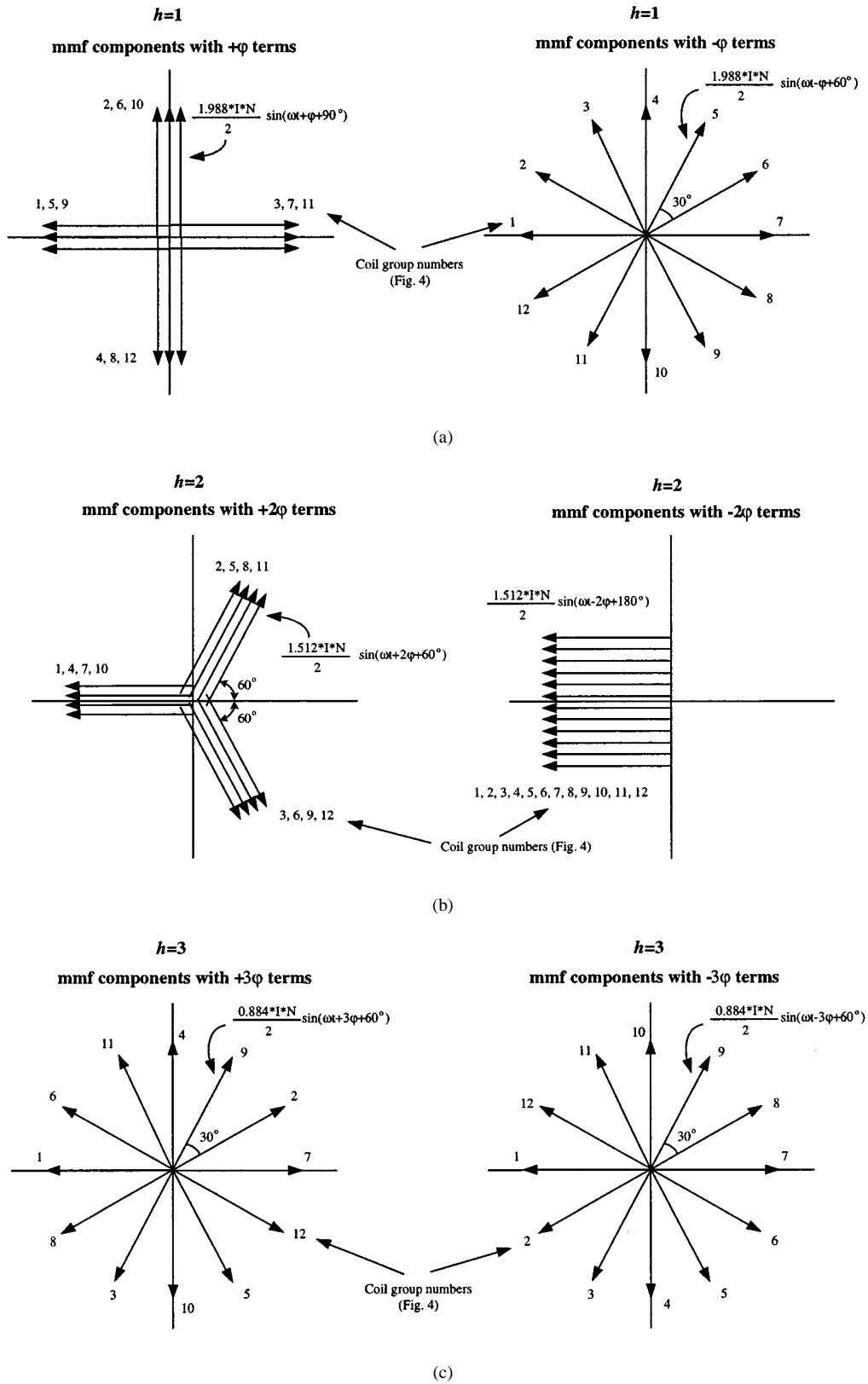


Fig. 6. The MMF vector components for each harmonic order h [see (10)]. The equations of some vectors are also shown in the diagrams as examples. (a) $h = 1$. (b) $h = 2$. (c) $h = 3$.

sating harmonic component at $h = 1$ [$+\varphi$ terms in Fig. 6(a)]. From Fig. 6(a) (by inspection) it can be concluded that by suitably phase shifting inverters 2 and 4 by $\pm 30^\circ$ the MMF harmonic component for $h = 1$, $+\varphi$ terms can be cancelled. The

consequence of phase shift of inverters 2 and 4 by $\pm 30^\circ$ will result in a decrease in the fundamental MMF component [$h = 2$, -2φ terms in Fig. 6(b)] by 9%. The simulation result in Fig. 9 discusses these aspects more in depth.

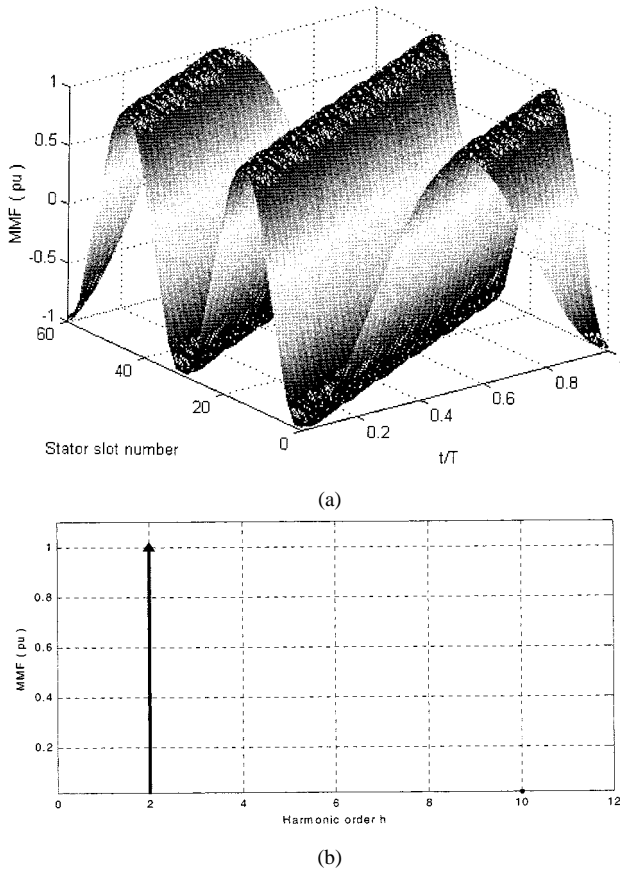


Fig. 7. (a) Three-dimensional MMF plot of the motor with all 12 coil groups energized. (b) The FFT components of the MMF wave in Fig. 7(a).

V. SIMULATION RESULTS

The MMF waveshape of the motor shown in Fig. 4 is simulated in MATLAB. Since a complete winding diagram of the motor is available, the MMF wave is computed by assuming six/12 lead connections with coil excitation currents in (8). This procedure is detailed in [10].

A. MMF Waveshape for Normal Condition

Fig. 7(a) shows the three-dimensional plot of the MMF wave when all coil groups are excited with a balanced set of currents. The x axis in Fig. 7(a) (t/T) represents the per-unit time where T is the period of currents in (8). Stator slot numbers are shown in the y axis in Fig. 7(a). The z axis is the MMF of the motor in p.u. We observe in Fig. 7(a) that the MMF wave has two cycles from slot 1 to slot 60 and it is nearly sinusoidal. Also, it is clear from Fig. 7(a) that the MMF wave rotates by time. Fig. 7(b) shows the Fourier components of the waveform in Fig. 7(a).

B. MMF Waveshape in 12-Lead Connection with One Faulted Delta Motor Winding

Fig. 3 shows the 12-lead connection. Now, if we assume inverter 1 is inoperative or coil groups 1, 5, 9 are not excited, the resulting MMF waveshape is shown in Fig. 8(a). From Fig. 8(b), the dominant MMF harmonic component is at $h = 1$ as predicted in Section IV-B. Further, in Section IV-C, it was shown that the MMF harmonic at $h = 1$ can be eliminated by phase shifting inverters 2 and 4 by $\pm 30^\circ$. Fig. 9(a) shows

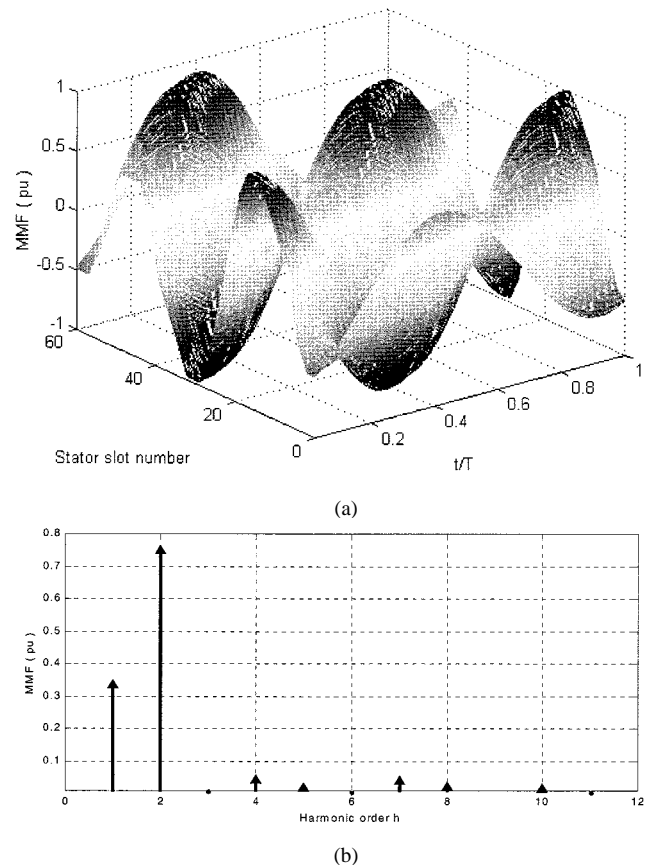


Fig. 8. (a) Three-dimensional plot of MMF of the motor connected in 12-lead connection and inverter 1 is inoperative (Fig. 3). (b) The FFT components of the MMF wave in Fig. 8(a).

the MMF wave resulting from this new operating condition. It is clear from Fig. 9(a) that the MMF ripple has decreased. Also, Fig. 9(b) shows that the MMF component for $h = 1$ is cancelled. However, phase shift of inverters 2 and 4 by $\pm 30^\circ$ results in derating of the inverter system as the magnitude of the MMF for $h = 2$ is reduced from 0.75 p.u. to 0.68 p.u.

C. MMF Waveshape in Six-Lead Connection with One Faulted Delta Motor Winding

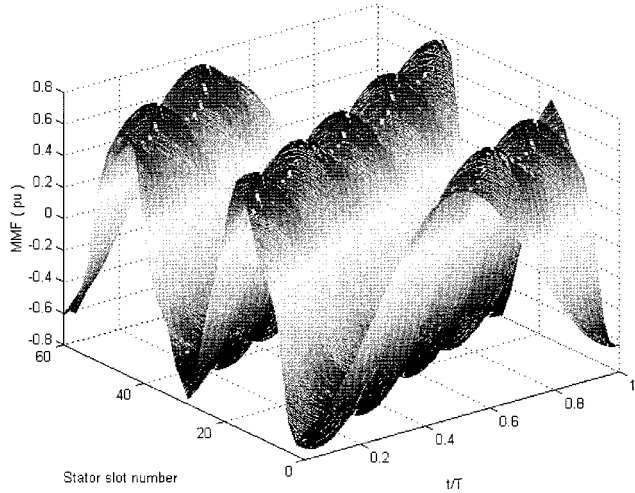
Fig. 2(b) shows the six-lead connection of the four-pole motor. Now, if we assume inverter 1 is inoperative or coil groups 1, 3, 5, 7, 9, 11 are not excited, the resulting MMF is shown in Fig. 10(a). The FFT of the MMF wave in Fig. 10(a) is shown in Fig. 10(b). Note that we have 0.5 p.u. fundamental MMF component ($h = 2$) since half of the motor winding is not energized.

VI. DESIGN EXAMPLE

In this section, a detailed design example of a 250-hp four-pole 60-Hz 2300-V/4160-V induction motor is discussed.

Motor Parameters:

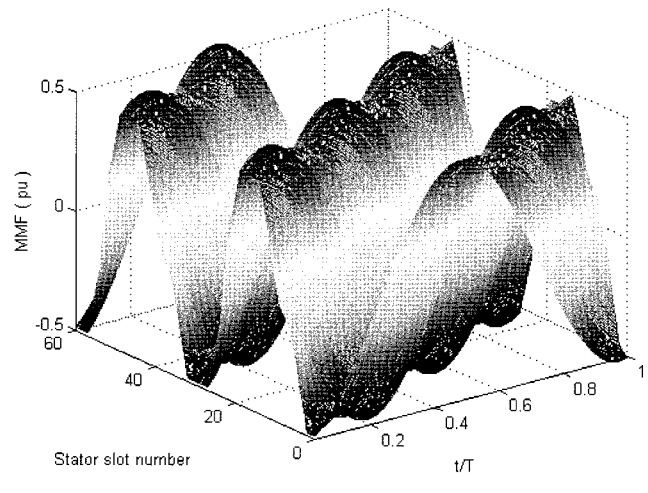
- power (P_o) = 250 hp;
- power factor (pf) = 0.8;
- efficiency (η) = 0.85;
- line-to-line voltage (V_{LL}) = 4160 V_{rms};
- fundamental output frequency (f_o) = 60 Hz.



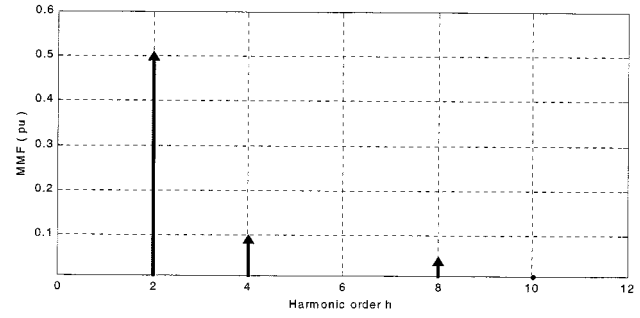
(a)



(b)



(a)



(b)

Fig. 9. (a) Three-dimensional MMF plot of the motor connected in 12-lead configuration (Fig. 3) and inverter 1 is inoperative. Also, output currents of inverter 2 are shifted by -30° and those of inverter 4 are shifted by $+30^\circ$. (b) The FFT components of the MMF wave in Fig. 9(a).

Fig. 10. (a) Three-dimensional plot of the MMF of the motor connected in six-lead connection; inverter 1 in Fig. 2(b) is inoperative. (b) The FFT components of the MMF wave in Fig. 10(a).

Apparent power (S) and motor current (I) in 4160-V connection [Fig. 1(b)] of the motor can be calculated as follows:

$$S = \frac{P_o}{\eta \cdot pf} = 275 \text{ kVA} \quad (12)$$

$$I = \frac{S}{\sqrt{3} \cdot V_{LL}} = 38 \text{ A.} \quad (13)$$

The voltage across each coil group V_a by (2) is

$$V_a = 600 \text{ V}_{\text{rms}}. \quad (14)$$

If the motor is connected in 12-lead (Fig. 3), the line-to-line output voltage of each three-phase inverter is the same as $V_a = 600 \text{ V}_{\text{rms}}$ and the output current of each three-phase inverter I_o is

$$I_o = \sqrt{3}I = 66 \text{ A}_{\text{rms}}. \quad (15)$$

The rms current of the insulated gate bipolar transistor (IGBT) and diode pairs in the three-phase inverters is

$$I_{sw, \text{rms}} = \frac{I_o}{\sqrt{2}} = 47 \text{ A}_{\text{rms}}. \quad (16)$$

The dc-bus voltage of each three-phase inverter V_{dc} is

$$V_{dc} = \frac{\sqrt{2} \cdot V_{LL}}{6m_a} = 850 \text{ V} \quad (17)$$

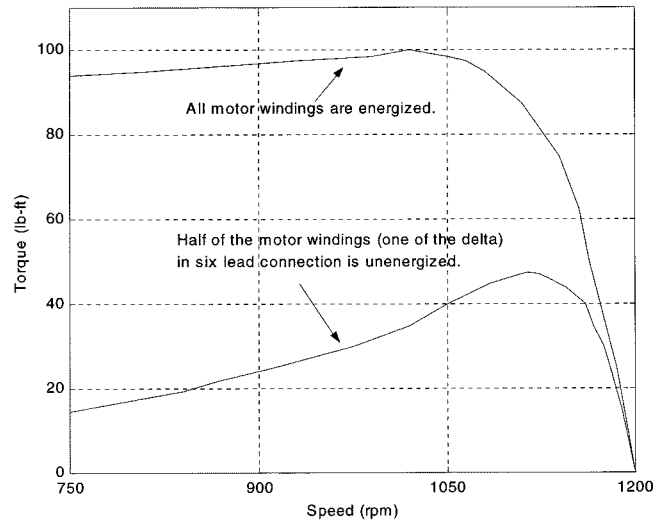


Fig. 11. Experimental torque–speed characteristic of the motor (see Table III in the Appendix) under full winding and half winding excitations. (The voltage across each coil group is its rated voltage at 60 Hz.)

where m_a is the modulation index and assumed 1.15 in (17). The IGBT's in the inverters are rated at rms current of 47 A. Further, IGBT's rated at 1700 V or higher can be employed in each inverter module to operate at a $V_{dc} = 850 \text{ V}$.

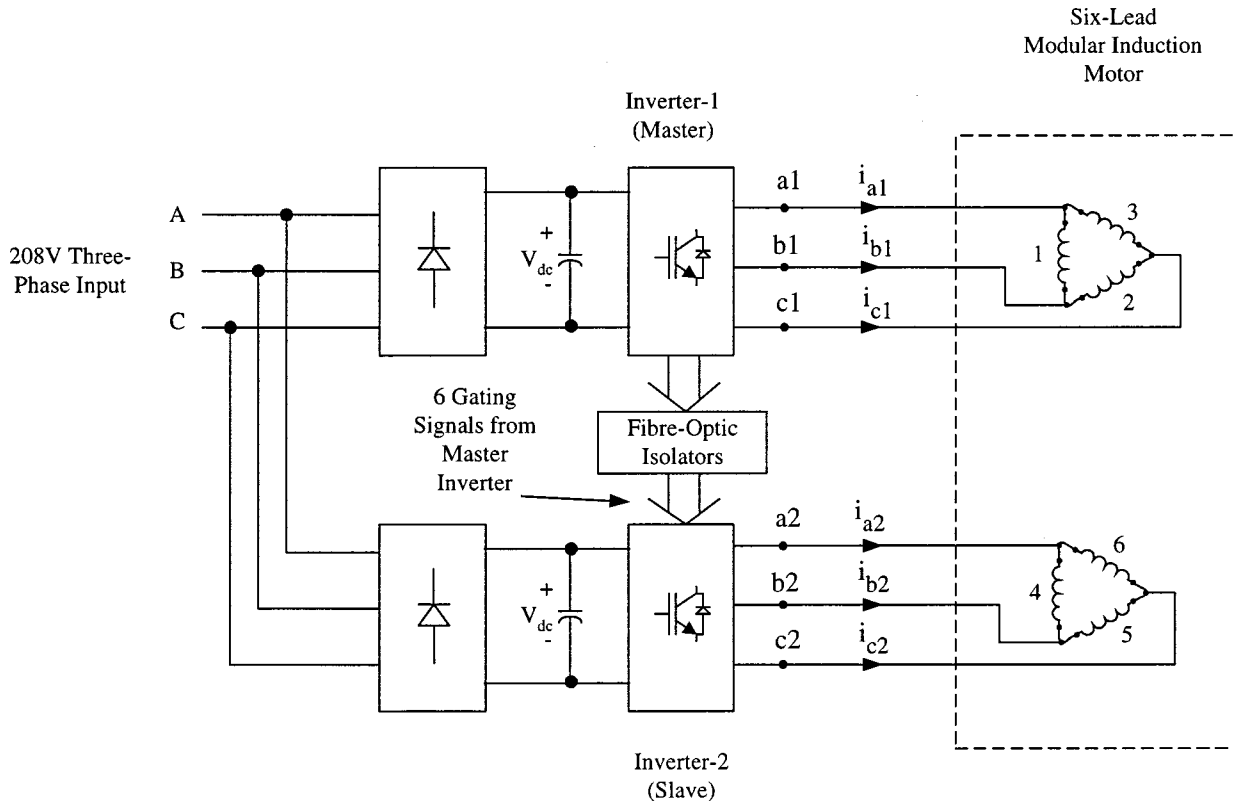


Fig. 12. The experimental setup of modular motor-modular inverter ASD. (The motor is six-pole and connected in six-lead configuration.)

The voltage stress between any winding groups do not exceed V_{dc} in Fig. 3. Therefore, the voltage insulation level of the motor is only 850 V. On the other hand, the maximum voltage that motor windings experience in the conventional connection of the motor [Fig. 1(b)] is the peak value of 4160 V, that is, 5900 V. The voltage insulation requirement of the motor has decreased from 5900 to 850 V (by 85.6%). This translates into significant cost saving and ease in manufacturing of the motor if the proposed concept is adopted. Further, the voltage insulation level of the three-phase inverters is also 850 V.

Now, if the motor is connected in six-lead configuration as shown in Fig. 2(b), we have

$$I_o = 132 \text{ A}_{\text{rms}}, \quad I_{sw, \text{rms}} = 94 \text{ A}_{\text{rms}} \quad \text{and} \quad V_{dc} = 850 \text{ V}.$$

VII. EXPERIMENTAL RESULTS

The proposed MM-MI concept is implemented on a laboratory prototype 230-V/460-V 60-Hz 10-hp six-pole motor, which is connected in six-lead configuration. The motor has 18 coil groups and Table II in the Appendix has additional details.

Both locked-rotor and breakdown torque tests were performed on the motor at 60 Hz. The test was repeated for both full winding (18 coil groups energized) and half winding (only nine coil groups energized.) The characteristics are plotted in Fig. 11. The breakdown torque of the motor under half-winding excitation is 47 lbf-ft, which is nearly half compared to the full-winding excitation (Fig. 11) Also, the motor slip for a given torque is slightly larger for half-winding excitation.

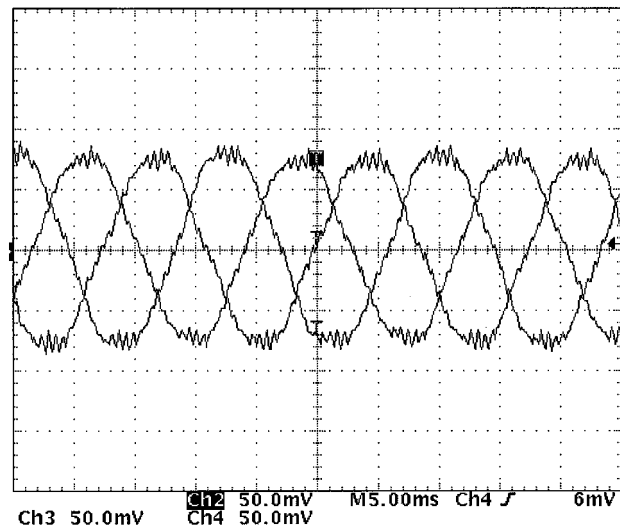


Fig. 13. Output currents of inverter 1: i_{a1} , i_{b1} , and i_{c1} . ($i_{a1} = i_{a2}$, $i_{b1} = i_{b2}$ and $i_{c1} = i_{c2}$.) Horizontal axis: 5 ms/div; vertical axis: 5 A/div.

The motor was then connected in six-lead configuration to run from two inverters operating in master/slave mode configuration (Fig. 12). Two commercially available inverters were modified for this purpose. Fig. 13 shows the motor currents i_{a1} , i_{b1} , and i_{c1} supplied by inverter 1 (Fig. 12). The inverter 2 currents are nearly identical. Fig. 14 shows the PWM output voltage of inverter 1. Fig. 15 shows the motor currents i_{a1} , i_{b1} , and i_{c1} when inverter 2 (slave) is shut down.

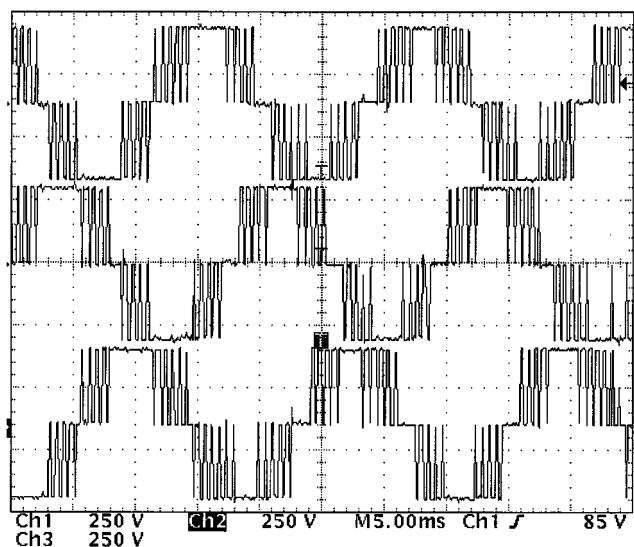


Fig. 14. Line-to-line output voltages of inverter 1: v_{a1b1} , v_{b1c1} , and v_{c1a1} . ($v_{a1b1} = v_{a2b2}$, $v_{b1c1} = v_{b2c2}$, and $v_{c1a1} = v_{c2a2}$.) Horizontal axis: 5 ms/div; vertical axis: 250 V/div.

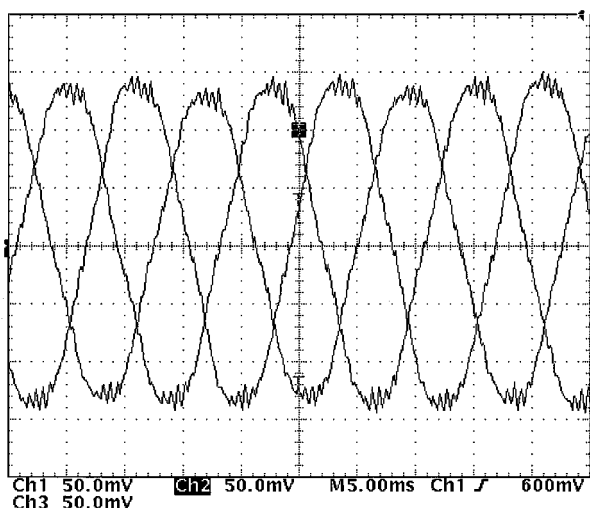


Fig. 15. The output currents of inverter 1: (i_{a1} , i_{b1} , and i_{c1}) while the slave inverter is shut down. Horizontal axis: 5 ms/div; vertical axis: 5 A/div.

VIII. CONCLUSIONS

In this paper a new MM-MI concept for MV-ASD systems has been introduced. It has been shown that standard MV motor winding connections can be reconnected into several three-phase groups, each powered by a separate three-phase PWM inverter, resulting in a high-performance MV-ASD system. The proposed approach is fault tolerant and can continue to operate at reduced power levels under inverter and/or motor faults. It has been shown that two three-phase inverters operating in master/slave configuration with a rated output voltage of 600 V are sufficient to power a 250-hp 4160-V four-pole 60-Hz motor. In the case of 12-lead connection, it has been shown that under inverter/motor faults, the remaining inverters can be suitably phase shifted to cancel MMF harmonics resulting from partial winding excitation. Experimental results

demonstrate the performance of a laboratory prototype 460-V 10-hp motor for the proposed six-lead connection.

APPENDIX

TABLE II
NAMEPLATE DATA OF THE MOTOR

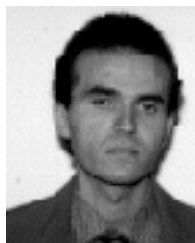
Volts: 230 / 460	Hp: 10	SF: 1.15
RPM: 1165	Poles: 6	NOM. F. L. EFF.: 88.5
AMP.: 27 / 13.5	Hz: 60	Ins. Class: F

TABLE III
LOCKED-ROTOR TEST RESULTS

	FULL WINDING	HALF WINDING
Voltage (V_{rms})	230	230
Current (A_{rms})	144.7	88.1
Power (kW)	34.6	21.45
Torque (lb-ft)	111.3	46.2

REFERENCES

- [1] "Adjustable speed drives—Application guide," Electric Power Research Institute, Palo Alto, CA, Rep. TR101140, 1992.
- [2] Siemens AG. Siemens medium voltage drives catalog. [Online]. Available: http://www2.ad.siemens.de/asi/frameset/e_f_asi1.html
- [3] Ansaldo Ross Hill. Medium voltage ASD's. [Online]. Available: <http://www.ansaldo.org>
- [4] General Electric. GE drive systems . [Online]. Available: <http://www.ge.com/gemis/ds0.htm>
- [5] ABB. Medium voltage ASD's. [Online]. Available: <http://www.abb.fi/vsd/mediamac.htm>
- [6] R. A. Hanna and S. Prabhu, "Medium voltage adjustable speed drives—Users' and manufacturers' experiences," *IEEE Trans. Ind. Applicat.*, vol. 33, pp. 1407–1415, Nov./Dec. 1997.
- [7] E. A. Klingshirn, "High phase order induction motors, Part II—Experimental results," *IEEE Trans. Power App. Syst.*, vol. PAS-102, pp. 54–59, Jan. 1983.
- [8] M. A. Abbas *et al.*, "Six-phase voltage source inverter driven induction motor," *IEEE Trans. Ind. Applicat.*, vol. IA-20, pp. 1251–1259, Sept./Oct. 1984.
- [9] T. M. Jahns, "Improved reliability in solid-state ac drives by means of multiple independent phase-drive units," *IEEE Trans. Ind. Applicat.*, vol. IA-16, pp. 321–331, May/June 1980.
- [10] V. Ostovic, *Computer-Aided Analysis of Electric Machines*. Englewood Cliffs, NJ: Prentice-Hall, 1994.
- [11] Texas A&M University System, College Station, TX, "Method and system for modular motor, modular inverter adjustable speed drive," U.S. Patent Application.
- [12] H. A. Toliyat, Course notes, ELEN-689, Elect. Eng. Dep., Texas A&M University, College Station.



Ekrem Cengelci (S'99) received the B.Sc. degree in electronics and telecommunication engineering from Yildiz Technical University, Istanbul, Turkey, and the M.S. degree in electric power engineering from Rensselaer Polytechnic Institute, Troy, NY, in 1993 and 1996, respectively. He is currently working toward the Ph.D. degree in power electronics at Texas A&M University, College Station.

His interest in power electronics is modular adjustable-speed-drive systems.

Mr. Cengelci received Second Prize Paper Awards from the Industrial Power Converter and Industrial Drives Committees of the IEEE Industry Applications Society in 1998 and 1999, respectively.



Prasad N. Enjeti (S'86–M'88–SM'95–F'00) received the B.E. degree from Osmania University, Hyderabad, India, the M.Tech degree from Indian Institute of Technology, Kanpur, India, and the Ph.D. degree from Concordia University, Montreal, PQ, Canada, in 1980, 1982, and 1988, respectively, all in electrical engineering.

In 1988, he joined the Department of Electrical Engineering, Texas A&M University, College Station, as an Assistant Professor. In 1994, he became an Associate Professor and, in 1998, a Professor. His primary

research interests are advance converters for power supplies and motor drives, power quality issues and active power filter development, utility interface issues, and "clean power" converter designs. He is the holder of two U.S. patents and has licensed two new technologies to industry. He is the Lead Developer of the Power Quality Laboratory at Texas A&M University and is actively involved in many projects with industry, while engaged in teaching, research, and consulting in the areas of power electronics, motor drives, power quality, and clean power utility interface issues.

Prof. Enjeti was the recipient of numerous IEEE Industry Applications Society (IAS) Best Paper Awards, the Second Best Paper Award for papers published in mid-year 1994 to mid-year 1995 from the IEEE TRANSACTIONS ON INDUSTRY APPLICATIONS, and the *IEEE Industry Applications Magazine* Prize Article Award in 1996. He is a member of the IAS Executive Board and Chair of the Standing Committee on Electronic Communications. He is a Registered Professional Engineer in the State of Texas.



James W. Gray (A'92) was born in Philadelphia, Mississippi. He received the B.Sc. degree from the University of Houston, Houston, TX.

He is currently an Assistant Chief Engineer with Toshiba International Corporation, Houston, TX. For the past 18 years with Toshiba International Corporation, he has been working with power electronics and rotating machines in the areas of research and development, product testing, and design, application, and manufacturing engineering.

Prior to joining Toshiba International Corporation, he spent 13 years with U.S. Electrical Motors, working with new product development, product testing, and design and manufacturing engineering. He has coauthored numerous papers on power quality and inverter applications.